



Synthesis, characterization and photoelectrochemical performance of a *tris*-heteroleptic ruthenium(II) complex having 4,7-dimethyl-1,10-phenanthroline



F. Carvalho, E. Liandra-Salvador, F. Bettanin, J.S. Souza, P. Homem-de-Mello, A.S. Polo*

Federal University of ABC, Av. dos Estados, 5001, Santo André 09210-580, Brazil

ARTICLE INFO

Article history:

Received 9 December 2013
Received in revised form 28 January 2014
Accepted 5 February 2014
Available online 14 February 2014

Keywords:

Molecular engineering
Dye-sensitized solar cells
tris-Heteroleptic ruthenium
DFT

ABSTRACT

The novel *cis*-[Ru(Me₂-phen)(dcbH₂)(NCS)₂] complex was prepared using a one-pot route and characterized based on ¹H NMR, FTIR, absorption and emission spectra. The properties of this complex were compared with those of *cis*-[Ru(R₂-phen)(dcbH₂)(NCS)₂], where R = Ph or H, to establish a relationship between the donor/acceptor character of the R substituent and the observed behavior of these compounds. Computational methods were also employed to gain a comprehensive understanding of this relationship. By using electron-donating/accepting substituents, it was possible to tune both the ground and excited states of the *cis*-[Ru(R₂-phen)(dcbH₂)(NCS)₂] complexes. This compound is capable of sensitizing the TiO₂ surface and efficiently converting the sunlight into electricity. In comparison to *cis*-[Ru(Ph₂-phen)(dcbH₂)(NCS)₂] it is observed that the presence of phenyl groups provide higher efficiency. The conversion efficiency was improved in comparison to *cis*-[Ru(phen)(dcbH₂)(NCS)₂]. This increase in efficiency is attributed to an increase in electron density, thus favoring electron transfer to TiO₂.

© 2014 Elsevier B.V. All rights reserved.

1. Introduction

tris-Heteroleptic ruthenium compounds, such as *cis*-[Ru(L)(L')(X)₂], where L ≠ L', are very interesting because their properties, in both the ground and excited states, can be modulated by the choice of the ligands. The preparation of these compounds is not simple, and several routes can be used to obtain the desired compound. These routes can start from Ru(DMSO)₄(Cl)₂ [1] or polymeric [Ru(CO)₂(Cl)₂]_n [2]. In early 2000s, a one-pot route using a dichloro(*p*-cymene)ruthenium(II) dimer was used to prepare a series of *tris*-heteroleptic ruthenium dye sensitizers, *cis*-[Ru(dRbpy)(dcbH₂)(NCS)₂] (bpy = 2,2'-bipyridine derivatives, R = methyl, nonyl, hexyl or tridecyl substituents) [3], and since this time, several similar compounds, *cis*-[Ru(L)(dcbH₂)(NCS)₂], L = 2,2'-bipyridine derivatives, have been prepared and investigated as sensitizers for use in dye-sensitized solar cells, DSSCs [4]. Among these complexes, the C101 complex [5], which has a thiophene derivative as the bipyridine substituents, exhibited better performance than *cis*-[Ru(dcbH₂)₂(NCS)₂], also known as N3,

and its *bis*-deprotonated analogue, N719, which are considered standards for these investigations. Density functional theory (DFT) has been successfully employed to describe the electronic properties of these compounds and to establish a relationship with their behavior as dye-sensitizers in DSSCs [6–14]. Few compounds have been prepared using other ligands similar to 2,2'-bipyridine, such as 1,10-phenanthroline.

Some *cis*-[Ru(L)(dcbH₂)(NCS)₂] compounds where L = 1,10-phenanthroline or its derivatives were prepared and evaluated as dye-sensitizers for DSSCs. Ligands including phen, dppz [15], 5,6-dimethyl-phen [16], Ph₂-phen [17] have been evaluated previously and, especially the complex having the Ph₂-phen ligand, exhibit a better performance than N719. However, there has been no investigation of the relationship between the electron donor or acceptor character of the ligand substituent and the properties of the ground and excited states of the complexes.

In this work, *cis*-[Ru(R₂-phen)(dcbH₂)(NCS)₂] complexes where R = Me, H or Ph, Fig. 1, were synthesized and characterized. The relationship between the R group and the donor or acceptor characteristics was evaluated based on their electronic properties determined by quantum chemistry as well as their FTIR, ¹H NMR, absorption and emission spectra. Their performances as dye-sensitizers for solar cells are also compared and discussed in terms of the phenanthroline substituents.

* Corresponding author. Tel.: +55 11 4996 0164; fax: +55 11 4996 0090.
E-mail address: andre.polo@ufabc.edu.br (A.S. Polo).

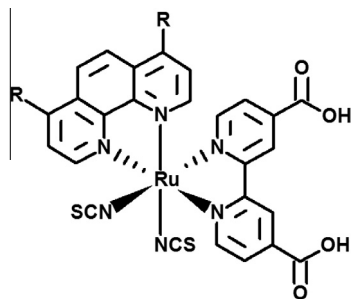


Fig. 1. Structure of the prepared compounds; R = Me, H or Ph.

2. Experimental details

4,4'-dimethyl-2,2'-bipyridine (Aldrich, 99%), H₂SO₄ (Sigma-Aldrich, 97%), [Ru(*p*-cymene)Cl₂]₂ (Aldrich), 1,10-phenanthroline, phen (Synth), 4,7-dimethyl-1,10-phenanthroline, Me₂-phen (Alfa Aesar, 98%), 4,7-diphenyl-1,10-phenanthroline, Ph₂-phen (Aldrich, 98%), a methanolic solution of tetrabutylammonium hydroxide (Acros Organics), Sephadex LH20 (Aldrich), N,N'-dimethylformamide-D₇, (Aldrich), NaNCS (Merck), Na₂Cr₂O₇ (Synth), HCl (Fluka), HNO₃ (Sigma-Aldrich), methanol (Synth), ethanol (Synth), isopropanol (Synth), N,N'-dimethylformamide, DMF (Synth), H₂PtCl₆ (Acros), fluorine-doped tin oxide (FTO – 8 ohm square⁻¹, Aldrich), the low temperature sealant – Surlyn (30 μm – Dyesol), acetonitrile (Lichrosolv – Merck), valeronitrile (HPLC – Aldrich), iodine (Sigma-Aldrich), guanidinium thiocyanate (Sigma-Aldrich) 4-*tert*-butylpyridine (Aldrich) and 1-butyl-3-methylimidazolium iodide (Aldrich) were used as received.

2.1. Synthesis of 2,2'-bipyridine-4,4'-dicarboxylic acid (dcbH₂)

The compound 2,2'-bipyridine-4,4'-dicarboxylic acid (dcbH₂) was synthesized as described in the literature [18]. Briefly, 1.60 g (8.6 mmol) of 4,4'-dimethyl-2,2'-bipyridine was added to a solution of 6.28 g (19.4 mmol) of Na₂Cr₂O₇ dissolved in 21 mL of concentrated H₂SO₄, and the mixture was stirred for 30 min. The resulting solution was added to 220 mL of cold water, and the solid was removed and dissolved in 10% NaOH. The final product was precipitated by the addition of HCl to the solution until it reached pH 2, and the white solid was collected. Yield: 70–80%. *Anal. Calc.* for C₁₂H₁₀N₂O₅: C, 57.60; H, 3.49; N, 11.20. *Found:* C, 57.84; H, 3.34; N, 11.27%.

2.2. Synthesis of *cis*-[Ru(R₂-phen)(dcbH₂)(NCS)₂]

The *tris*-heteroleptic complexes were synthesized using the procedure reported in the literature with slight modifications [15,17]. In general, the ruthenium *p*-cymene dimer, [Ru(*p*-cymene)Cl₂]₂, was added to N,N'-dimethylformamide (DMF) and 2 equivalents of (R₂-phen) was added. The mixture was kept at 80 °C for 2 h under an inert atmosphere. After this period, 2 equivalents of dcbH₂ was added to the mixture, and the temperature was increased to 160 °C. The mixture was kept at this temperature for 4 h. Finally, NaNCS was added to the mixture in a 10-fold excess, and the reaction was kept under these conditions for 4 h to allow the reaction to proceed to completion. All the reactions were monitored by UV–Vis spectrophotometry and thin layer chromatography (silica gel, 60 Å, as the stationary phase and methanol saturated with NaCl as the eluent). To obtain pure compounds, the complexes were deprotonated using a methanolic solution of tetrabutylammonium hydroxide (1 mol L⁻¹), centrifuged to remove any residual particulates and applied to a liquid chromatog-

raphy column containing Sephadex LH-20 as the stationary phase. Methanol was used as the eluent. The pure fraction was concentrated, precipitated by the addition of HNO₃ and filtered, and the solid was dried in a desiccator.

Using this procedure, it was possible to prepare *cis*-[Ru(phen)(dcbH₂)(NCS)₂] (yield = 78%; *Anal. Calc.* for C₂₆H₂₁N₆O₇RuS₂: C, 44.83; H, 3.49; N, 12.31. *Found:* C, 44.95; H, 3.05; N, 12.10%), *cis*-[Ru(Ph₂-phen)(dcbH₂)(NCS)₂] (yield = 65%; *Anal. Calc.* for C₅₀H₄₄N₈O₁₁RuS₂: C, 57.49; H, 3.05; N, 10.59. *Found:* C, 57.18; H, 4.11; N, 9.63%) and *cis*-[Ru(Me₂-phen)(dcbH₂)(NCS)₂] (yield = 76%; *Anal. Calc.* for C₂₈H₂₆N₆O₇RuS₂: C, 46.38; H, 3.54; N, 11.53. *Found:* C, 46.47; H, 3.62; N, 11.6%).

2.3. Dye-sensitized solar cells

Dye-sensitized solar cells were prepared in a sandwich-type arrangement, as shown in Fig. 2. Nanocrystalline TiO₂ mesoporous films were prepared as described elsewhere [19] and deposited onto FTO conducting glasses to provide an active area of 0.16 cm² and sintered for 30 min at 450 °C. The films were sensitized by immersing the processed electrodes into an ethanolic solution of each prepared compound for a minimum duration of 12 h. The counter-electrodes have a thin film of platinum as a catalyst layer on their conductive sides. The solar cells were sealed using a film of sealant, and the mediator was placed between photoanode and counter-electrode through holes made on the counter-electrodes. The mediator was prepared by dissolving iodine (76 mg), guanidinium thiocyanate (118 mg), 4-*tert*-butylpyridine (0.76 mL) and 1-butyl-3-methylimidazolium iodide (1.60 g) in a mixture of acetonitrile:valeronitrile (85:15) to produce a solution with a final volume of 10 mL.

2.4. Methods

NMR spectra were recorded at 25.0 °C on a DRX-500 Bruker Avance spectrometer at 500.13 MHz using DMF-D₇ as the solvent.

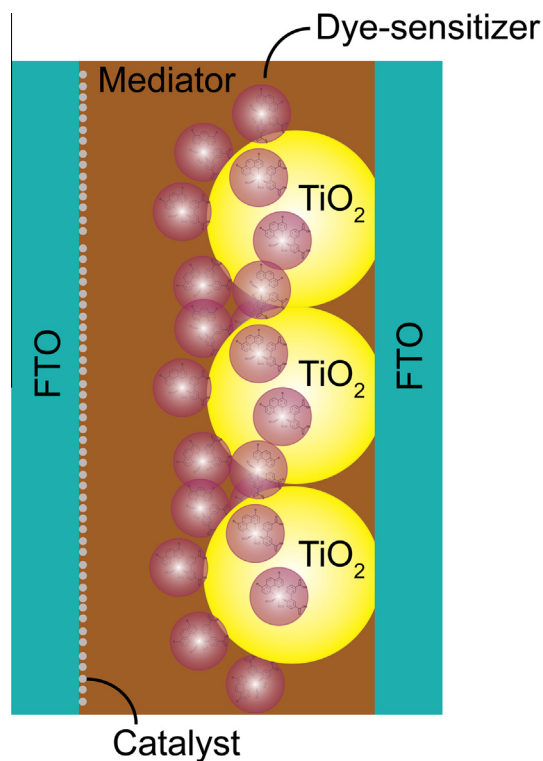


Fig. 2. Schematic representation of a dye-sensitized solar cell.

The residual DMF peaks were used as an internal standard. FTIR spectra were recorded at 25.0 °C in KBr pellets on a Bomem MB 100 spectrometer (4 cm⁻¹ resolution). Electronic absorption spectra were recorded on an Agilent 8453 diode-array spectrophotometer using quartz cuvettes with a 1.000 cm path length. Uncorrected emission spectra were recorded on a Cary Eclipse spectrofluorimeter using quartz cuvettes with a 1.000 cm path length after the samples had been purged with argon. Photocurrent action spectra were obtained using a Newport system. This system consists of a 300 W Xe lamp (model 6258) placed in a lamp housing that illuminates the entrance slit of a 0.25 m Czerny–Turner monochromator (Cornerstone 260), which has a diffraction grating of 1200 lines mm⁻¹ and band-pass filters to avoid second-order effects. The quasi-monochromatic light beam exits the monochromator, and a beam-splitter splits the incident light to the sample and a silicon detector, model 818-UV, which was connected to a virtual power-meter, model 841-p-USB. The photocurrent was measured using a Keithley – 2410 source-meter. Current–potential curves were obtained by measuring the current response for the applied voltage provided by a Keithley – 2410 source-meter, from 0 V to the open-circuit photovoltage, under simulated solar irradiation. The incident light was provided by a Newport solar simulator, model 96000, using a 150 W Xe lamp (6255) placed in a lamp housing. The housing includes a water filter to remove the near IR region and a filter to provide the simulated A.M. 1.5G solar spectrum. The intensity was measured using a thermopile detector, model 818P-001-12, connected to a power-meter, model 842-PE. The results presented for the photoelectrochemical experiments are the average of at least 5 distinct experiments.

2.5. Computational details

The computational calculations employed the B3LYP [20–23] functional to obtain geometries and vibrational spectra and, in the time-dependent implementation, to obtain absorption spectra. Several studies have used the same functional to obtain geometries

[10–14,24–26] and simulate the vibrational and electronic spectra of ruthenium complexes [12–14,26,27]. The absence of imaginary frequencies ensures that the structures obtained correspond to minima in the potential energy surfaces. TD-DFT simulations were performed for 80 states.

All calculations were performed with the LANL2DZ [28–30] basis set as implemented in the GAUSSIAN 09 [31] package. Solvation effects (acetonitrile) were introduced in all calculations with the Integral Equation Formalism of the Polarizable Continuum Model (IEFPCM) [32–37] using the GAUSSIAN 03 defaults.

3. Results

3.1. ¹H NMR spectra

The proton signals of the *tris*-heteroleptic compounds in the ¹H NMR spectra were difficult to distinguish because both ligands exhibit signals in the same region, from 10 to 7 ppm. To avoid misinterpretation, H–H COSY bidimensional correlation experiments were performed for *cis*-[Ru(Me₂-phen)(dcbH₂)(NCS)₂], Fig. 3. The assignments for *cis*-[Ru(phen)(dcbH₂)(NCS)₂] and *cis*-[Ru(Ph₂-phen)(dcbH₂)(NCS)₂] were based on this interpretation as well as their coupling constants and on their previous assignments described in the literature [15,17], Table 1.

The protons of the aromatic rings *trans* to NCS were shifted upfield in comparison to the protons of the aromatic rings that were *trans* to each other, as shown by the data listed in Table 1. This effect was attributed to the anisotropic effect, resulting in the shielding of these protons.

3.2. FTIR

The FTIR spectra of *cis*-[Ru(R₂-phen)(dcbH₂)(NCS)₂], Fig. 4, exhibit peaks in the aromatic region, from 1650 to 1410 cm⁻¹, which were attributed to the ν(CC) and ν(CN) of the aromatic ligands [38]; however, it was not possible to distinguish their characteristic

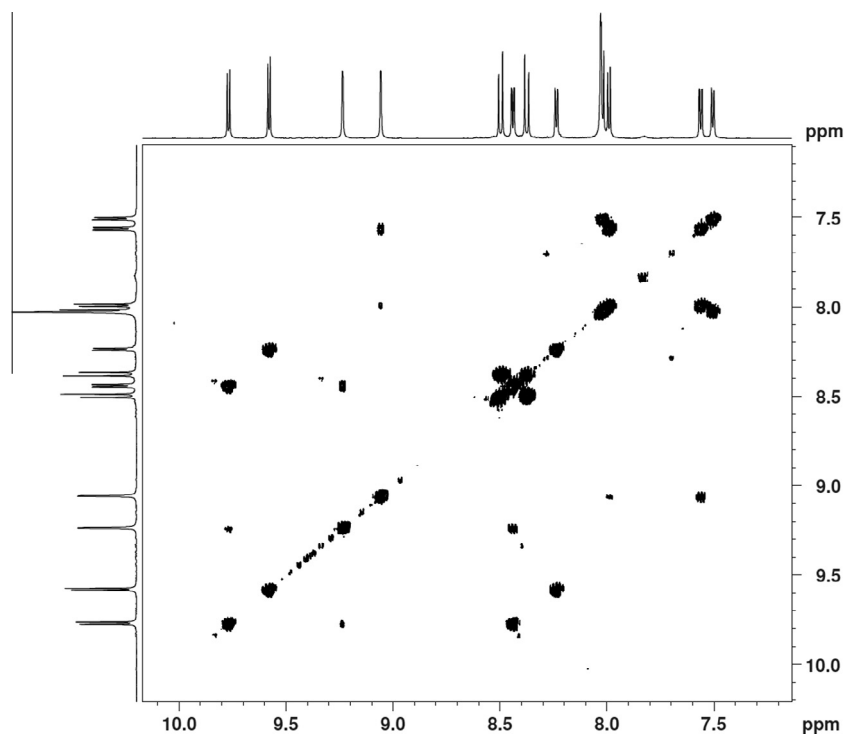


Fig. 3. H–H COSY bidimensional NMR spectrum of *cis*-[Ru(Me₂-phen)(dcbH₂)(NCS)₂] in DMF-d₇. (500 MHz).

Table 1
Chemical structure and ^1H NMR chemical shifts (δ) and coupling constants (J) for the protons of $\text{cis-}[\text{Ru}(\text{Me}_2\text{-phen})(\text{dcbH}_2)(\text{NCS})_2]$, (DMF-d^7 ; 500 MHz).

Proton type	δ (ppm)	J (Hz)
H_a (d, 1H)	9.77	5.8
H_b (d, 1H)	8.44	5.8
H_c (s, 1H)	9.24	
H_d (s, 1H)	9.06	
H_e (d, 1H)	7.56	6.0
H_f (d, 1H)	7.99	6.0
H_2 (d, 1H)	9.58	5.3
H_3 (d, 1H)	8.24	5.3
H_5 (d, 1H)	8.02	5.5
H_6 (d, 1H)	7.51	5.5
H_8 (d, 1H)	8.37	9.3
H_9 (d, 1H)	8.50	9.3

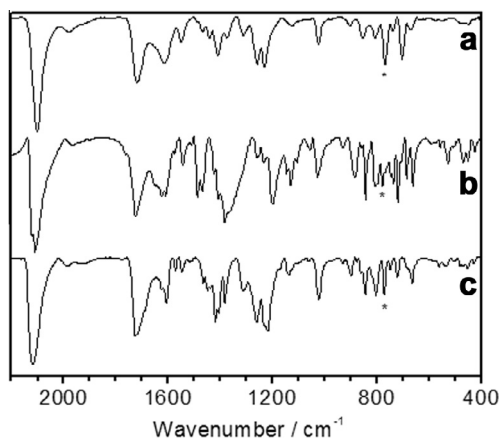


Fig. 4. FTIR spectra of $\text{cis-}[\text{Ru}(\text{R}_2\text{-phen})(\text{dcbH}_2)(\text{NCS})_2]$, $\text{R} = \text{Ph}$ (a), H (b) or Me (c), in KBr. (* indicates the peak ascribed to the NCS peak at 770 cm^{-1}).

signals. The distinct $\nu(\text{CO})$ of the carboxylic groups of the dcbH_2 ligand were observed in all spectra between 1740 and 1715 cm^{-1} .

FTIR is a valuable tool to evaluate the presence of N or S linkage isomers of $\text{cis-}[\text{Ru}(\text{R}_2\text{-phen})(\text{dcbH}_2)(\text{NCS})_2]$ because the coordination of the NCS^- ion through the N or S atom results in stretches with distinct maxima. Special attention was given to CN stretching, $\nu(\text{NCS})$, which can be observed in the 2100 and 770 cm^{-1} regions.

Only one peak was observed for each complex in both regions due to the existence of only $\text{cis-}[\text{Ru}(\text{R}_2\text{-phen})(\text{dcbH}_2)(\text{NCS})_2]$ complexes. The existence of both isomers would be indicated by peaks at 2100 and 770 cm^{-1} as well as 2050 and 700 cm^{-1} , ascribed to coordination through nitrogen and sulfur, respectively [39,40]. The FTIR spectra of the prepared complexes exhibited only one peak, indicating that the isothiocyanate isomer was the main product [41].

The isothiocyanate peaks were observed at 2101 and 770 cm^{-1} for $\text{cis-}[\text{Ru}(\text{Ph}_2\text{-phen})(\text{dcbH}_2)(\text{NCS})_2]^{2-}$, at 2109 and 780 cm^{-1} for $\text{cis-}[\text{Ru}(\text{phen})(\text{dcbH}_2)(\text{NCS})_2]$ and at 2117 and 771 cm^{-1} for $\text{cis-}[\text{Ru}(\text{Me}_2\text{-phen})(\text{dcbH}_2)(\text{NCS})_2]$. The simulation of the IR spectra gave frequencies for the symmetric stretching of the NCS ligand of 2130.1 , 2130.5 and 2131.0 cm^{-1} for $\text{R} = \text{Ph}$, H and Me , respectively, in $\text{cis-}[\text{Ru}(\text{R}_2\text{-phen})(\text{dcbH}_2)(\text{NCS})_2]$.

3.3. Absorption spectra

The $\text{cis-}[\text{Ru}(\text{R}_2\text{-phen})(\text{dcbH}_2)(\text{NCS})_2]$ compounds exhibited two absorption bands with high molar absorptivity ($\approx 10^4\text{ L mol}^{-1}\text{ cm}^{-1}$) in the visible region ($350\text{--}700\text{ nm}$), Fig. 5. These absorption

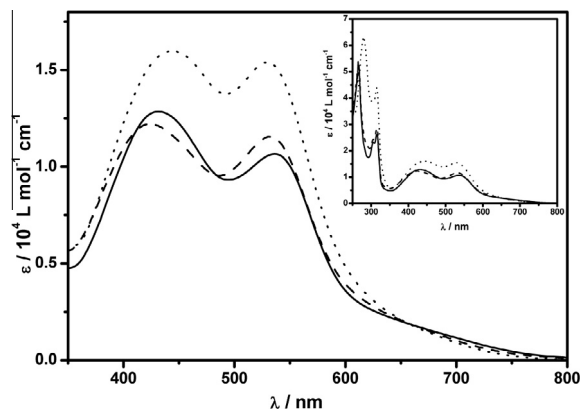


Fig. 5. Absorption spectra of $\text{cis-}[\text{Ru}(\text{R}_2\text{-phen})(\text{dcbH}_2)(\text{NCS})_2]$, $\text{R} = \text{Me}$ (—), H (---) or Ph (···), in acetonitrile.

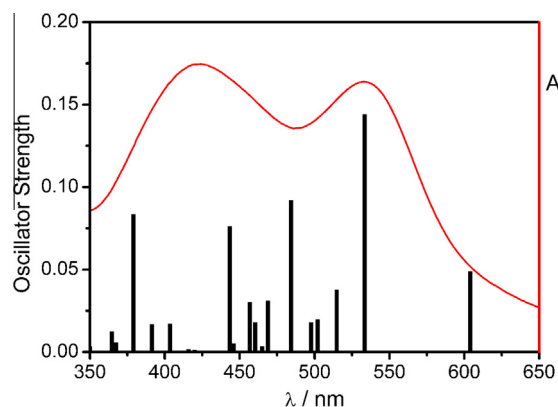


Fig. 6. Theoretical lines determined by TD-B3LYP/LanL2DZ/IEFPCM and experimental (—) absorption spectra for $\text{cis-}[\text{Ru}(\text{Me}_2\text{-phen})(\text{dcbH}_2)(\text{NCS})_2]$ in acetonitrile.

bands were primarily attributed to charge transfer transitions, and the peaks in the UV region were attributed to the internal electronic transitions of the ligands. These absorption features are typical of ruthenium polypyridyl complexes [15,17].

The $\text{cis-}[\text{Ru}(\text{Ph}_2\text{-phen})(\text{dcbH}_2)(\text{NCS})_2]$ complex exhibited two maxima, at 445 and 530 nm . For $\text{cis-}[\text{Ru}(\text{phen})(\text{dcbH}_2)(\text{NCS})_2]$, these peaks were centered at 420 and 530 nm , whereas for $\text{cis-}[\text{Ru}(\text{Me}_2\text{-phen})(\text{dcbH}_2)(\text{NCS})_2]$, the peaks were observed at 430 and 535 nm .

The TD-DFT peaks can be grouped into sets that resemble the experimental absorption bands, Fig. 6, with contributions to an absorption band in the ultraviolet region and two absorption bands in the visible range.

3.4. Emission spectra

The emission spectra of the complexes in acetonitrile exhibited broad and non-structured profiles, which are typical of $^3\text{MLCT}$ transitions, Fig. 7. These characteristics have also been observed for similar compounds [15,17].

The emission maxima for $\text{cis-}[\text{Ru}(\text{Ph}_2\text{-phen})(\text{dcbH}_2)(\text{NCS})_2]$, $\text{cis-}[\text{Ru}(\text{phen})(\text{dcbH}_2)(\text{NCS})_2]$ and $\text{cis-}[\text{Ru}(\text{Me}_2\text{-phen})(\text{dcbH}_2)(\text{NCS})_2]$ were at 755 , 790 and 805 , respectively.

3.5. Computational analyses

DFT calculations were performed for geometry optimization, followed by the simulation of the FTIR spectra, electrostatic surface potentials and electronic absorption spectra.

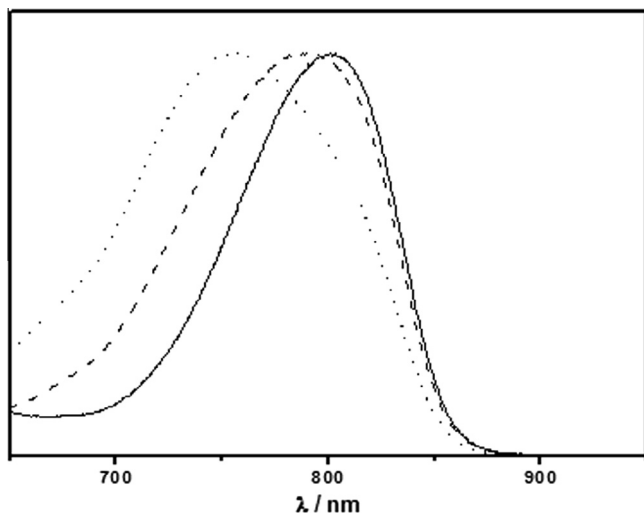


Fig. 7. Emission spectra of *cis*-[Ru(R₂-phen)(dcbH₂)(NCS)₂], R = Me (—); H (---) or Ph (···), in acetonitrile. ($\lambda_{\text{ex}} = 500 \text{ nm}$; $\nu = 30 \text{ nm min}^{-1}$).

Octahedral-like structures were found as the minima for the potential energy surfaces after the geometry optimization calculation for each compound, Fig. 8.

The electrostatic potential surfaces for the three compounds were calculated, and the results are presented in Fig. 9.

The charge distributions for all atoms are presented in the Supporting Info.

3.6. Photoelectrochemical experiments

The performances of these compounds as dye-sensitizers for solar cells were evaluated using current–voltage (*J*–*V*) curves, Fig. 10, and using photocurrent action spectra, Fig. 11. The photoelectro-

chemical parameters determined from these experiments are listed in Table 2.

The photoelectrochemical experiments demonstrate that the synthesized compounds have energy levels that are adequate for promoting electron injection into the semiconductor conducting band of TiO₂, converting the sunlight into electrical output. It is also observed that the presence of phenyl or methyl substituents on the phenanthroline ring enhances the performance of the solar cells. This performance increase is evident in both the overall efficiency and IPCE_{Max} when compared to the unsubstituted phenanthroline ring.

4. Discussion

The influence of the R groups at the 4 and 7 positions of the phenanthroline ligand on the properties of *cis*-[Ru(R₂-phen)(dcbH₂)(-NCS)₂] are notable and are related to their electron donor (methyl) or acceptor (phenyl) character. The values of the R group's Hammett constants and their main spectroscopic signals are listed in Table 3.

The influence of the R groups on the ¹H NMR spectrum can be primarily observed on δ_2 . The observed upfield shift in the order of Ph, H and Me is consistent with the increase in the electron donation character of the substituents. There was a correlation between the presence of the electron-withdrawing group (phenyl) and a decrease in the electron density of the aromatic rings, thus deshielding H₂ and shifting the signal downfield relative to that for phen. In contrast, the electron donation caused by methyl groups increased the electron density of the aromatic ring, shielding H₂ and resulted in the signal being shifted upfield. The electron density changes caused by the R groups did not have significant influences on long-range protons signals, such as that for H_a, as there was no correlation observed for their electron donor/acceptor character. The electron density was also evaluated using DFT calculations. The calculated atomic charges derived from the

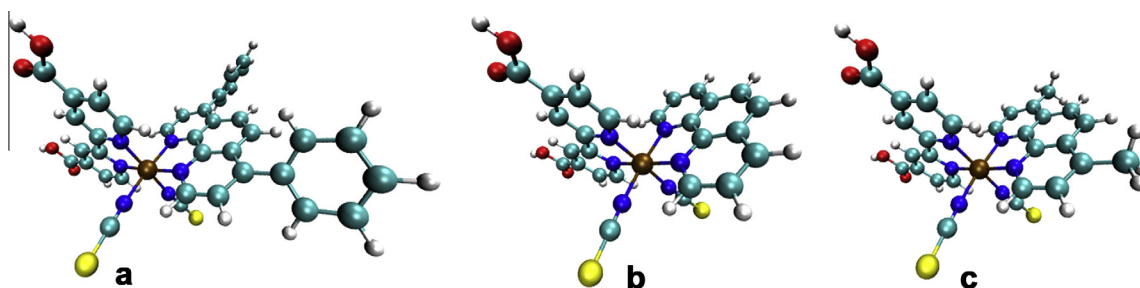


Fig. 8. Optimized quantum mechanics structures for *cis*-[Ru(R₂-phen)(dcbH₂)(NCS)₂]; R = Ph (a), H (b) or Me (c). (cyan = carbon, blue = nitrogen, red = oxygen, white = hydrogen, yellow = sulfur, brown = ruthenium). (For interpretation of the references to colour in this figure legend, the reader is referred to the web version of this article.)

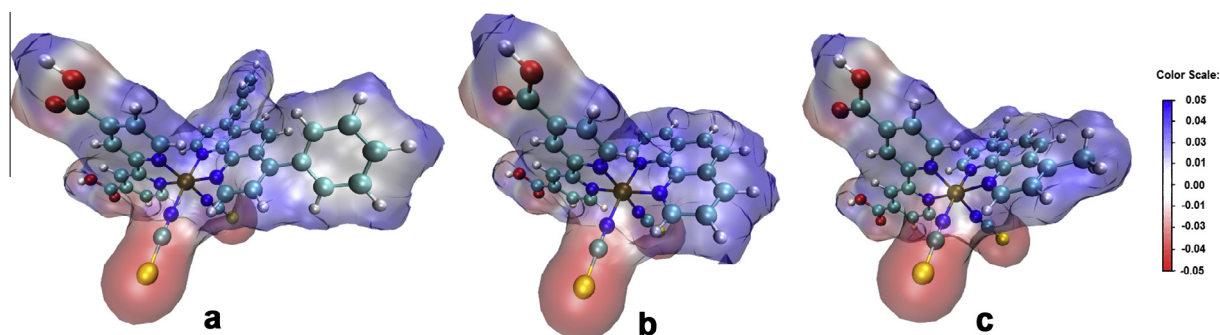


Fig. 9. Electrostatic surface potentials determined for *cis*-[Ru(R₂-phen)(dcbH₂)(NCS)₂]; R = Ph (a), H (b) or Me (c).[42,43].

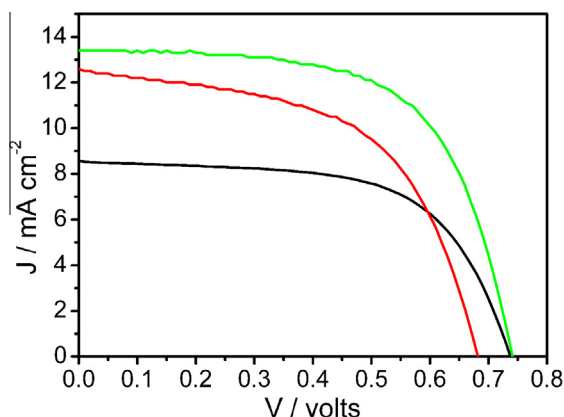


Fig. 10. Current–potential curves determined for DSSCs in which the photoanode was sensitized by *cis*-[Ru(R₂-phen)(dcbH₂)(NCS)₂], R = H (—); Me (—) or Ph (—).

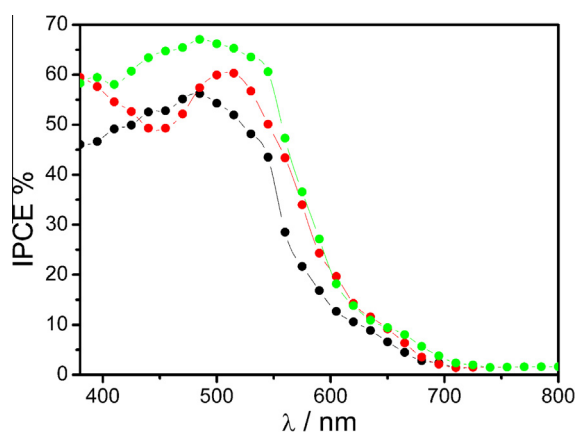


Fig. 11. Photocurrent action spectra of solar cells in which the photoanode was sensitized by *cis*-[Ru(R₂-phen)(dcbH₂)(NCS)₂], R = H (●); Me (●) or Ph (●).

electrostatic potential (ChelpG) for the three compounds, Table 4, confirmed the ¹H NMR observations: the electron density of the aromatic rings of phen increased in the order Ph < H < Me. The atomic charges on the nitrogen atoms of phen, N3 and N4, show that these atoms had higher electron densities as the donor character of R increased. The effect also extended to the N atoms of the opposite ligand: N1 and N6. The atomic charges on N2 and N5 were less affected.

The distinct characteristics of the R groups also resulted in changes in the ν(CN) stretching due to changes in the electron density of the metal center. It is interesting to note that the changes in ν(CN) are in accordance with the distinct electron donor/acceptor character of the R groups. The presence of phenyl groups in *cis*-[Ru(Ph₂-phen)(dcbH₂)(NCS)₂] resulted in a shift of 8 cm⁻¹ to a lower energy in comparison with the signal for the *cis*-[Ru(phen)(dcbH₂)(NCS)₂] complex. This electron withdrawing substituent on phenanthroline decreases the electronic density on ruthenium center and as a consequence, the electron donation of NCS⁻ ligand through the N–Ru σ bond is enhanced as well as its π interaction to t_{2g}^{*}, and weak the CN bond as can be observed

Table 3

Hammett constants for the R substituents and the main spectroscopic signals of these substituents determined for *cis*-[Ru(R₂-phen)(dcbH₂)(NCS)₂].

	Ph	H	Me
σ _p [44]	0.05	0	-0.14
δ _a (ppm)	9.80	9.71	9.77
δ _z (ppm)	9.85	9.74	9.58
ν _(NCS) (cm ⁻¹)	2101; 770	2109; 780	2117; 770
λ _{max-abs} (nm)	445; 535	420; 530	430; 535
λ _{max-em} (nm)	755	790	805

Table 4

ChelpG charges determined for the nitrogen atoms of the investigated compounds (L = R₂-phen; R = Ph, H or Me).

	Ph	H	Me	
	N1	0.261	0.215	0.187
	N2	-0.116	-0.117	-0.113
	N3	-0.258	-0.273	-0.370
	N4	0.255	0.207	0.112
	N5	-0.222	-0.261	-0.250
	N6	-0.308	-0.360	-0.377

on FTIR shift. In contrast, the presence of methyl groups in *cis*-[Ru(Me₂-phen)(dcbH₂)(NCS)₂] resulted in a shift of 8 cm⁻¹ to a higher energy region in comparison with the signal for *cis*-[Ru(phen)(dcbH₂)(NCS)₂] due to their electron donor character which results in the opposite effect. The calculated data for the NCS symmetric stretch are in agreement with the trend observed in the experimental data and can be explained by the change in the electron density due to distinct effect of the substituents.

A low influence of the R groups was observed for the lower energy absorption maxima of the compounds because the electronic transitions responsible for these absorption bands are primarily CT_{NCS-dcbH₂} [45], which are not directly connected to the R substituent. Thus, the energies of these electronic transitions are not sensitive to characteristics of the R group. Higher molar absorptivity values in the visible region were observed for *cis*-[Ru(Ph₂-phen)(dcbH₂)(NCS)₂] due to the presence of phenyl groups, which increased the light harvesting by this compound [17].

Theoretical calculations show that both bands in the visible region have MLCT character, Fig. 12. In some transitions, the most likely charge transfer is to dcbH₂, and in others, it is to R₂-phen. Transfers to R₂-phen have smaller oscillator strengths and are more important for transitions below 480 nm, corresponding to the absorption band in the higher energy region of the experimental spectra. The second band in the visible region is primarily due to transfers to dcbH₂. Because the molecular orbitals of the R₂-phen ligand are not directly involved, the calculations suggest an association between the inductive effect of the R group and the wavelength/intensity of the band. However, this difference was not observed in the experimental spectra because these absorption bands are broad, and the difference may have been too small to be detected.

Using different substituents in polypyridinic ligands leads to changes on the emission spectra of homoleptic ruthenium(II) poly-

Table 2

Photoelectrochemical parameters determined for solar cells sensitized by *cis*-[Ru(R₂-phen)(dcbH₂)(NCS)₂]; R = Ph, H or Me.

R	V _{oc} (Volts)	J _{sc} (mA cm ⁻²)	P _{max} (mW cm ⁻²)	ff	η (%)	IPCE _{max} (%) (λ (nm))
Ph	0.738	13.28	6.20	0.63	6.18	67 (485)
H	0.733	8.67	3.88	0.61	3.78	56 (485)
Me	0.683	12.72	4.73	0.55	4.60	60 (515)

pyridyl complexes since these complexes have the $^3\text{MLCT}$ as the lowest lying excited state and the use of electron donor or acceptor substituent changes both the HOMO and LUMO of these compounds, leading to an increase or decrease on emission energy. An interesting behavior was observed for the emission properties of the $\text{cis-}[\text{Ru}(\text{R}_2\text{-phen})(\text{dcbH}_2)(\text{NCS})_2]$ complexes investigated. The emission energy increased as the electron-withdrawing character increased. This apparent contradictory effect can be explained by the presence of the $^3\text{MLCT}_{\text{dRu-}\pi^*\text{dcbH}_2}$ thexi (*thermally equilibrated excited*) state for all the complexes presented. In this case, the thexi state energy is almost the same for all compounds investigated, while the electron-withdrawing effect of the phenyl groups reduces the electron density at the metal center, and consequently, reduces the energy of its HOMO, resulting in the observed increase in energy. In contrast, the donor effect of the methyl groups changes the energy of its HOMO to higher energy and reduces the energy observed for emission from this state.

The photoelectrochemical performance of the solar cells is improved by the presence of the methyl electron donor group. These results are consistent with those from the other experiments that were performed. This substituent increases the electron density on dcbH_2 , which led to a shift of the photocurrent action spectrum to a lower energy region when compared to $\text{cis-}[\text{Ru}(\text{phen})(\text{dcbH}_2)(\text{NCS})_2]$. Since the ratio between the integrated photocurrent action spectra of $\text{cis-}[\text{Ru}(\text{Me}_2\text{-phen})(\text{dcbH}_2)(\text{NCS})_2]$ and $\text{cis-}[\text{Ru}(\text{phen})(\text{dcbH}_2)(\text{NCS})_2]$ is 1.14 and the ratio of their J_{SC} is 1.47, are quite similar under the experimental conditions, the improvement in the overall performance of the DSSCs can be ascribed to the shift on the photocurrent action spectrum of $\text{cis-}[\text{Ru}(\text{Me}_2\text{-phen})(\text{dcbH}_2)(\text{NCS})_2]$.

The use of phenyl substituents also improves the performance of the prepared solar cells. This behavior is apparently in contrast

to the previous discussion. It is expected that the performance of solar cells should be lower due to the presence of an electron-withdrawing substituent on the phenanthroline ring. However, valuable information is obtained from the photocurrent action spectra. In these spectra, an increase in performance is observed for the $\text{cis-}[\text{Ru}(\text{Ph}_2\text{-phen})(\text{dcbH}_2)(\text{NCS})_2]$ compound in the 380–600 nm region in comparison to other compounds.

The IPCE can be expressed as a function of the electron-injection quantum efficiency, Φ_{EI} ; the efficiency of collecting electrons in the external circuit, η_{EC} ; and the light harvesting efficiency, LHE, at a determined wavelength. These terms have the mathematical relationship described by Eq. (1) [4].

$$\text{IPCE}(\lambda)\Phi_{\text{EI}} \cdot \eta_{\text{EC}} \cdot \text{LHE} \quad (1)$$

The Φ_{EI} can be considered constant for all dyes since the same anchoring group was used for the compounds investigated. The unexpected performance of $\text{cis-}[\text{Ru}(\text{Ph}_2\text{-phen})(\text{dcbH}_2)(\text{NCS})_2]$ can be attributed to its higher molar absorptivity values when compared to the other compounds, Fig. 5, and to a lower recombination of the injected electron. It was already observed the influence of electron donor or acceptor groups on charge recombination dynamics in DSSCs, which can enhance the performance of the device [46]. Thus, the presence of phenyl groups on phenanthroline ligand can enhance both LHE and η_{EC} terms and further investigation is being carried out.

5. Conclusion

The new *tris*-heteroleptic $\text{cis-}[\text{Ru}(\text{Me}_2\text{-phen})(\text{dcbH}_2)(\text{NCS})_2]$ complex was synthesized, characterized and compared with other phenanthroline complexes with substituents with distinct characters. The results indicate that the R substituents of the phenanthroline ligands affect some of the characteristics of the ground and excited states of $\text{cis-}[\text{Ru}(\text{R}_2\text{-phen})(\text{dcbH}_2)(\text{NCS})_2]$. The ^1H NMR, FTIR and emission experiments were found to depend on the acceptor or donor character of the R groups. The calculated absorption spectrum resembled the experimental spectrum, allowing the comprehensive interpretation of the absorption spectra of these complexes. The calculated atomic charges demonstrated that the inductive effects involve one nitrogen atom of the dcbH_2 ligand in the sequence Ph, H and Me, thus explaining the sequence observed for the experimental ^1H NMR and FTIR data and demonstrating a viable way to tune the properties of $\text{cis-}[\text{Ru}(\text{R}_2\text{-phen})(\text{dcbH}_2)(\text{NCS})_2]$. The photoelectrochemical performance of the compounds as dye sensitizers were evaluated, and it was observed that the improvement in the performance of the solar cells was due to electronic effects of methyl groups. The use of phenyl groups revealed that the light-harvesting efficiency or the reduction on electron recombination of this dye has more influence on the performance of DSSCs than its electron-withdrawing effects.

Acknowledgments

The authors would like to acknowledge FAPESP (2011/11717-8 and 2007/05370-0), UFABC and CAPES for financial support.

Appendix A. Supplementary material

Supplementary data associated with this article can be found, in the online version, at <http://dx.doi.org/10.1016/j.ica.2014.02.002>.

References

- [1] K. Hara, H. Sugihara, Y. Tachibana, A. Islam, M. Yanagida, K. Sayama, H. Arakawa, G. Fujihashi, T. Horiguchi, T. Kinoshita, *Langmuir* 17 (2001) 5992.

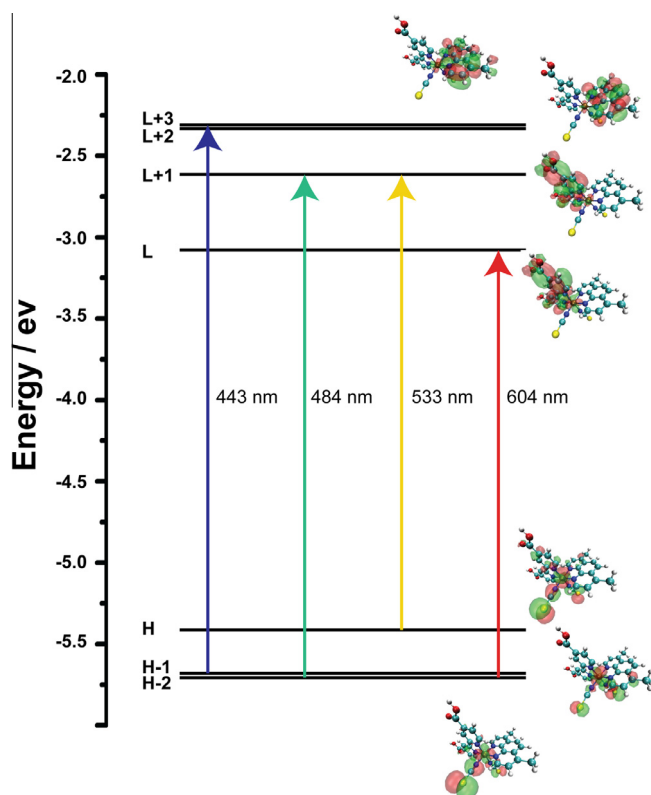


Fig. 12. Schematic representation of selected electronic transitions and the molecular orbitals involved in the absorption spectrum of $\text{cis-}[\text{Ru}(\text{Me}_2\text{-phen})(\text{dcbH}_2)(\text{NCS})_2]$.

- [2] M.J. Nickita, A.I. Belousoff, A.M. Bhatt, G.B. Bond, G. Deacon, L. Gasser, *Inorg. Chem.* 46 (2007) 8638.
- [3] M.K. Nazeeruddin, S.M. Zakeeruddin, J.J. Lagref, P. Liska, P. Comte, C. Barolo, G. Viscardi, K. Schenk, M. Graetzel, *Coord. Chem. Rev.* 248 (2004) 1317.
- [4] J.S. Souza, L.O.M. Andrade, A.S. Polo, *Nanomaterials for solar energy conversion: Dye-sensitized solar cells based on ruthenium(II) tris-heteroleptic compounds or natural dyes*, in: F.L. Souza, E.R. Leite (Eds.), *Nanoenergy: Nanotechnology Applied for Energy Production*, Springer, 2012, pp. 49–80.
- [5] F. Gao, Y. Wang, D. Shi, J. Zhang, M. Wang, X. Jing, R. Humphry-Baker, P. Wang, S.M. Zakeeruddin, M. Grätzel, *J. Am. Chem. Soc.* 130 (2008) 10720.
- [6] S. Fantacci, F. De Angelis, A. Selloni, *J. Am. Chem. Soc.* 125 (2003) 4381.
- [7] F. Aiga, T. Tada, *Sol. Energy Mater. Sol. Cells* 85 (2005) 437.
- [8] F. Aiga, T. Tada, *J. Mol. Struct.* 658 (2003) 25.
- [9] V. Barone, F.F. de Biani, E. Ruiz, B. Sieklucka, *J. Am. Chem. Soc.* 123 (2001) 10742.
- [10] F. Dumur, C.R. Mayer, K. Hoang-Thi, I. Ledoux-Rak, F. Miomandre, G. Clavier, E. Dumas, R. Meallet-Renault, M. Frigoli, J. Zyss, F. Secheresse, *Inorg. Chem.* 48 (2009) 8120.
- [11] F. De Angelis, S. Fantacci, A. Selloni, *Chem. Phys. Lett.* 389 (2004) 204.
- [12] F. De Angelis, S. Fantacci, A. Selloni, M.K. Nazeeruddin, *Chem. Phys. Lett.* 415 (2005) 115.
- [13] J.E. Monat, J.H. Rodriguez, J.K. McCusker, *J. Phys. Chem. A* 106 (2002) 7399.
- [14] M.K. Nazeeruddin, F. De Angelis, S. Fantacci, A. Selloni, G. Viscardi, P. Liska, S. Ito, T. Bessho, M. Graetzel, *J. Am. Chem. Soc.* 127 (2005) 16835.
- [15] N. Onozawa-Komatsuzaki, O. Kitao, M. Yanagida, Y. Himeda, H. Sugihara, K. Kasuga, *New J. Chem.* 30 (2006) 689.
- [16] A. Reynal, A. Forneli, E. Martinez-Ferrero, A. Sanchez-Diaz, A. Vidal-Ferran, E. Palomares, *Eur. J. Inorg. Chem.* 2008 (2008) 1955.
- [17] Y.L. Sun, A.C. Onicha, M. Myahkostupov, F.N. Castellano, *Acs Appl. Mater. Interfaces* 2 (2010) 2039.
- [18] C.L. Donnici, D.H. Maximo, L.L.C. Moreira, G.T. dos Reis, E.F. Cordeiro, I.M.F. de Oliveira, S. Carvalho, E.B. Paniago, *J. Braz. Chem. Soc.* 9 (1998) 455.
- [19] A.S. Polo, N.Y. Murakami Iha, *Sol. Energy Mater. Sol. Cells* 90 (2006) 1936–1944.
- [20] B. Miehlich, A. Savin, H. Stoll, H. Preuss, *Chem. Phys. Lett.* 157 (1989) 200.
- [21] A.D. Becke, *J. Chem. Phys.* 98 (1993) 5648.
- [22] A.D. Becke, *Phys. Rev. A* 38 (1988) 3098.
- [23] C.T. Lee, W.T. Yang, R.G. Parr, *Phys. Rev. B* 37 (1988) 785.
- [24] D. Ambrosek, P.F. Loos, X. Assfeld, C. Daniel, *J. Inorg. Biochem.* 104 (2010) 893.
- [25] M. Al-Noaimi, B.F. Ali, A.M. Rawashdeh, Z. Judeh, *Polyhedron* 29 (2010) 3214.
- [26] K. Christopoulos, K. Karidi, A. Tsipis, A. Garoufis, *Inorg. Chem. Commun.* 11 (2008) 1341.
- [27] F. De Angelis, S. Fantacci, A. Selloni, M. Gratzel, M.K. Nazeeruddin, *Nano Lett.* 7 (2007) 3189.
- [28] W.R. Wadt, P.J. Hay, *J. Chem. Phys.* 82 (1985) 284.
- [29] P.J. Hay, W.R. Wadt, *J. Chem. Phys.* 82 (1985) 299.
- [30] P.J. Hay, W.R. Wadt, *J. Chem. Phys.* 82 (1985) 270.
- [31] M.J. Frisch, G.W. Trucks, H.B. Schlegel, G.E. Scuseria, M.A. Robb, J.R. Cheeseman, J.A. Montgomery, T. Vreven, K.N. Kudin, J.C. Burant, J.M. Millam, S.S. Iyengar, J. Tomasi, V. Barone, B. Mennucci, M. Cossi, G. Scalmani, N. Rega, G.A. Petersson, H. Nakatsuji, M. Hada, M. Ehara, K. Toyota, R. Fukuda, J. Hasegawa, M. Ishida, T. Nakajima, Y. Honda, O. Kitao, H. Nakai, M. Klene, X. Li, J.E. Knox, H.P. Hratchian, J.B. Cross, V. Bakken, C. Adamo, J. Jaramillo, R. Gomperts, R.E. Stratmann, O. Yazyev, A.J. Austin, R. Cammi, C. Pomelli, J.W. Ochterski, P.Y. Ayala, K. Morokuma, G.A. Voth, P. Salvador, J.J. Dannenberg, V.G. Zakrzewski, S. Dapprich, A.D. Daniels, M.C. Strain, O. Farkas, D.K. Malick, A.D. Rabuck, K. Raghavachari, J.B. Foresman, J.V. Ortiz, Q. Cui, A.G. Baboul, S. Clifford, J. Cioslowski, B.B. Stefanov, G. Liu, A. Liashenko, P. Piskorz, I. Komaromi, R.L. Martin, D.J. Fox, T. Keith, A. Laham, C.Y. Peng, A. Nanayakkara, M. Challacombe, P.M.W. Gill, B. Johnson, W. Chen, M.W. Wong, C. Gonzalez, J.A. Pople, in *Gaussian 09 v. A.02*, 2009.
- [32] M. Cossi, V. Barone, B. Mennucci, J. Tomasi, *Chem. Phys. Lett.* 286 (1998) 253.
- [33] M. Cossi, V. Barone, R. Cammi, J. Tomasi, *Chem. Phys. Lett.* 255 (1996) 327.
- [34] E. Cancès, B. Mennucci, J. Tomasi, *J. Chem. Phys.* 107 (1997) 3032.
- [35] B. Mennucci, E. Cancès, J. Tomasi, *J. Phys. Chem. B* 101 (1997) 10506.
- [36] B. Mennucci, J. Tomasi, *J. Chem. Phys.* 106 (1997) 5151.
- [37] J. Tomasi, B. Mennucci, E. Cancès, *Theochem-J. Mol. Struct.* 464 (1999) 211.
- [38] R.M. Silverstein, F.X. Webster, D.J. Kiemle, *Spectrometric Identification of Organic Compounds*, seventh ed., John Wiley & Sons, Hoboken, NJ, 2005.
- [39] A.H. Norbury, *Coordination chemistry of the cyanate, thiocyanate, and selenocyanate ions*, in: H.J. Emeléus, A.G. Sharpe (Eds.), *Advances in Inorganic Chemistry and Radiochemistry*, Academic Press, 1975, pp. 231–386.
- [40] K. Nakamoto, *Infrared and Raman Spectra of Inorganic and Coordination Compounds*, John Wiley & Sons Inc, New York, 1997.
- [41] M.K. Nazeeruddin, S.M. Zakeeruddin, K. Kalyanasundaram, *J. Phys. Chem.* 97 (1993) 9607.
- [42] W. Humphrey, A. Dalke, K. Schulten, *J. Molec. Graphics* 14 (1996) 33.
- [43] W. Humphrey, A. Dalke, K. Schulten, *VMD – Visual Molecular Dynamics*, 2012.
- [44] M. Smith, J. March, *March's Advanced Organic Chemistry: Reactions, Mechanisms, and Structure*, sixth ed., Wiley, Hoboken, USA, 2007.
- [45] M.K. Nazeeruddin, A. Kay, I. Rodicio, R. Humphry-Baker, E. Müller, P. Liska, N. Vlachopoulos, M. Grätzel, *J. Am. Chem. Soc.* 115 (1993) 6382.
- [46] A. Reynal, A. Forneli, E. Martinez-Ferrero, A. Sánchez-Díaz, A. Vidal-Ferran, B.C. O'Regan, E. Palomares, *J. Am. Chem. Soc.* 130 (2008) 13558.